

# Thin Alloy Zone Crystallisation

D. T. J. HURLE, J. B. MULLIN, E. R. PIKE

*Ministry of Aviation, Royal Radar Establishment, Great Malvern, Worcs, UK*

*Received 26 September 1966*

The basic principles of a family of crystal-growing techniques in which crystallisation of a substance is achieved via diffusion through a thin alloy zone (TAZ) from a third phase (solid, liquid, or vapour) are described. Crystallisation is achieved by the application of a gradient of a thermodynamic potential across the zone and various methods of establishing such a gradient are considered.

A theory predicting the velocity of a TAZ along a solid charge, published previously (D. T. J. Hurle, J. B. Mullin, and E. R. Pike, *Phil. Mag.* **9** (1964) 423), is extended to include the case where one of the solid phases is metastable. Expressions for the gradient of constitutional supercooling in the zone are derived for conventional and thin alloy zone crystallisation (TAZC) processes. It is shown that the important advantage in the use of a TAZ is the dramatic reduction in the supercooling at a given velocity compared to conventional processes.

A rationalisation of various published techniques of crystal growth within the concepts of TAZC is presented and some existing and potential applications of TAZC processes are reviewed.

## 1. Introduction

Thin Alloy Zone Crystallisation (TAZC) is a term used by the authors Hurle, Mullin, and Pike [1, 2] to refer to the family of crystal-growing techniques which are characterised by the following common features:

- (a) Crystallisation of a single-crystal solid phase ( $P_1$ ) is achieved via diffusion through a liquid alloy\* zone (L) – at least one dimension of which is small ( $\sim 25\mu\text{m}$ ) – from a third phase ( $P_2$ ).
- (b) The liquid alloy zone acts as a solvent and transport medium for the material being crystallised.
- (c) The driving force for crystallisation is a difference in free energy between phase  $P_1$  and  $P_2$ .

The geometry of the liquid zone can be spherical, cylindrical (motion of the zone normal to the axis of the cylinder), or lamellar (motion of the zone perpendicular to the plane). The following discussion will be concerned principally with the lamellar geometry.

A classification of TAZC processes based on the thermodynamic driving forces which can be used to achieve crystallisation from a liquid alloy zone has provided a useful framework for the rationalisation of existing techniques of crystal growth. This classification, which is considered in sections 3 and 5, has also enabled the prediction of new techniques.

A theoretical analysis of a TAZ moving under the influence of several thermodynamic driving forces is developed in section 4, and an expression for the steady velocity of the zone is derived. Subsequently, expressions for the gradient of constitutional supercooling during growth are derived for both TAZC and conventional processes. These results show that the potent advantage of TAZC techniques is the dramatic reduction in the gradient of constitutional supercooling in the melt during growth which occurs when the zone thickness is made very small.

However, before considering in detail the principles of TAZC, it is essential to consider

\*The phrase *liquid alloy* is used in its widest sense and includes all those liquid mixtures commonly referred to as solutions or fluxes (see for example reference 3).

the concept of constitutional supercooling and its significance in crystallisation from liquid alloy systems.

## 2. Crystallisation from Alloy Melts

The growth of good crystals from alloy melts is not normally achieved by vertical pulling or equivalent, fast crystallisation techniques (growth rate  $\sim 1$  cm/h). Crystallisation from alloy melts, such as, for example, germanium from gallium or aluminium solutions [4], yttrium iron garnet from a barium oxide-boric oxide flux (=alloy) [5], or barium titanate from potassium fluoride [6], is generally carried out by slow cooling of the liquid with or without a seed crystal being present or, alternatively, by maintaining the seed and source material at different temperatures within the liquid. In the latter method (Trumbore's thermal-gradient technique [4]), the source is maintained at a higher temperature than the seed and a steady transfer of the material to be crystallised takes place through the liquid from source to seed, i.e. down the temperature gradient.

It is not generally appreciated, however, in this and similar techniques, that growth necessarily occurs under conditions of constitutional supercooling. This can readily be appreciated with reference to fig. 1. In the steady state, the distribution of the solvent concentration will be as shown in fig. 1a and the corresponding liquidus temperature will be as shown in fig. 1b. If a condition of thermodynamic equilibrium (actual temperature equals liquidus temperature) holds at both solid/liquid interfaces, source and seed, and if there is an approximately linear temperature distribution in the liquid, then it is evident from fig. 1 that the whole of the liquid is constitutionally supercooled.

A consequence of alloy growth, therefore, is that crystals frequently show features indicative of cellular growth. Germanium crystals grown from gallium, for example, have been shown by Trumbore [4] to develop with octahedral (111) surfaces. It is reasonable to assume that a seed of arbitrary shape will develop a cellular structure as it grows, with consequent liquid-trapping in the cell boundary grooves. Further, if the crystal is allowed to grow freely into the solution, it will ultimately be bounded by slow-growing (111) planes with no re-entrant corners (fig. 2). This follows as a consequence of the increase in cell size which occurs with the increase in the

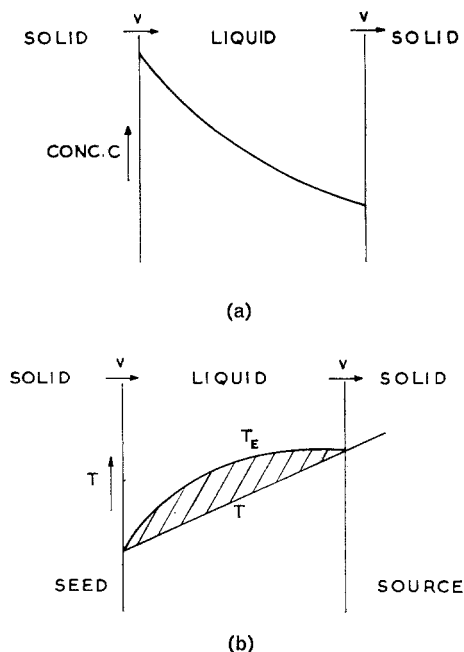


Figure 1 Concentration and temperature distributions in a moving alloy zone, illustrating the occurrence of constitutional supercooling.

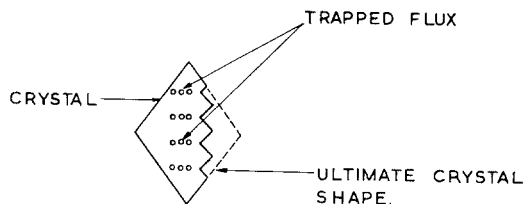


Figure 2 Diagrammatic representation of a flux-grown crystal showing cellular structure with droplets of trapped flux.

gradient of constitutional supercooling  $(dS/dx)_{x=0}$  as growth proceeds [7, 8]. Thereafter, provided the gradient of constitutional supercooling is not greater than that which the (111) surfaces can withstand, the crystal (germanium) will grow as an octahedron.

In general, crystals which develop habit faces do so when growing under conditions of constitutional supercooling. As a seed crystal of arbitrary shape grows out to its final shape, determined by these habit faces, cellular growth with solute trapping [8] occurs on the non-habit faces. This phenomenon is well known.

In practice, only a small temperature gradient can be imposed if crystals free from liquid trapping are to be grown. This is due, we think,

to the increase in  $(dS/dx)_{x=0}$  which occurs with increase in the temperature gradient. In diffusion-controlled systems, the rate of growth is proportional to the temperature gradient and hence only slow rates of growth ( $\sim 1$  mm/day) can be achieved without flux trapping.

### 3. Principles of TAZC

A disadvantage of conventional alloy-growth techniques, therefore, is the slow growth rate which is generally necessary to avoid flux trapping. This growth rate may be 1000 times slower than the growth rate which is suitable for the melt growth of pure materials. In theory, the potent advantage of confining the liquid alloy to a thin zone, normal to the direction of growth, as in TAZC techniques, is that the gradient of constitutional supercooling is much smaller for a given velocity than for large liquid zones as in conventional alloy growth. In practice, crystal growth by TAZC techniques which avoid flux trapping can approach the growth rates used for pure materials. The quantitative derivation of the gradient of constitutional supercooling and its dependence on growth and zone thickness for various alloy-growth techniques are discussed in section 4.2.

The driving force for zone motion can be described as the establishment of a gradient of thermodynamic potential across the thin liquid zone. For small driving forces, the zone velocity is proportional to the driving force—the gradient of chemical potential  $(\nabla\mu)$  or the gradient of electrochemical potential  $(\nabla\tilde{\mu})$  across the thin liquid zone. The electrochemical potential  $\tilde{\mu}$  can be written as  $\tilde{\mu} = \mu(p, T, \phi, c_1, \dots, c_n)$ , where  $p, T, \phi, c_1, \dots, c_n$  are the state variables of pressure, temperature, electrostatic potential, and concentration of the  $n$  components, respectively. By considering situations in which all but one of the variables are constant, it is possible to characterise all the principal TAZC techniques. These are shown in table I.

The phase which is consumed as the growth proceeds ( $P_2$ )—hereafter called the “charge”—can of course be a solid, liquid, or vapour. In existing processes, the charge is commonly a solid, but we show below that processes in which it is a liquid or vapour are also possible.

We would also remark that it is, of course, possible for the phase of the thin “alloy” zone to be solid, liquid, or vapour. The phenomenon of constitutional supercooling can, in principle, also occur in solid or vapour phases, but such

TABLE I Thermodynamic driving forces for zone motion.

Driving force	Equivalent	Description
$(\nabla\mu)_{p,c_1 \dots c_n}$	$\nabla T$	Temperature gradient zone melting (Temperature gradient TAZC)
$(\nabla\mu)_{T,c_1 \dots c_n}$	$\nabla p$	Pressure gradient TAZC
$(\nabla\tilde{\mu})_{p,T,c_1 \dots c_n}$	$\nabla\phi$	Direct-current induced TAZC
$(\nabla\mu)_{T,p,c_1 \dots c_{n-1}}$	$\nabla\mu_n$	Metastable phase TAZC

effects have not, to date, been investigated in detail. The occurrence of constitutional supercooling in the crystal growth of iodine from the vapour phase has recently been briefly reported by Reed and LaFleur [46].

The principles of specific TAZC processes will now be considered individually in more detail.

#### 3.1. Temperature Gradient TAZC

##### 3.1.1. Solid-Liquid-Solid (SLS) Process (Temperature Gradient Zone Melting)

The TGZM technique invented by Pfann [9, 10] is discussed in detail in his book [11]. Essentially, the relative particle flow of the components of the liquid alloy results from the concentration gradients of the components in the zone; these are a consequence of the difference in actual temperature between the two solid/liquid interfaces. Thus, with reference to figs. 4 and 5, the application of a temperature gradient which establishes interface temperatures of  $T(-L)$  and  $T(+L)$  results in motion of the interfaces in order to maintain the interface concentrations  $c(-L)$  and  $c(+L)$  respectively.

##### 3.1.2. Liquid-Liquid-Solid Processes

The LLS TAZC technique is a development of an idea originally proposed by Delves [12] for the use of immiscible liquids as a means of avoiding constitutional supercooling. The concept can be appreciated by considering fig. 3, which is a schematic representation of the region of the Hg-Te system involving immiscible liquids.

M is the monotectic point. If a liquid of composition  $c_Y$  is cooled below the liquidus temperature  $T_Y$ , two liquids  $L_1$  and  $L_2$  form; at a temperature  $T_x$  their compositions would be given by  $c_{Lx1}$  and  $c_{Lx2}$ . At the monotectic

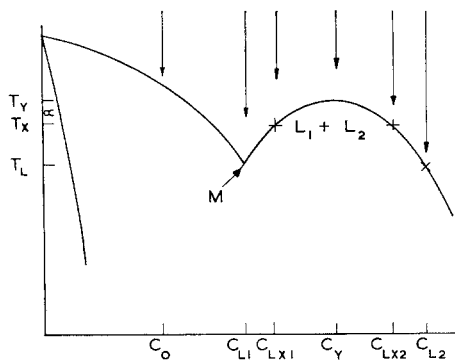


Figure 3 Phase diagram of a binary system with immiscible liquids (e.g. Hg-Te).

temperature  $T_L$ , solid  $\alpha$ , liquid  $c_{L1}$  and liquid  $c_{L2}$  co-exist in equilibrium. All the liquid  $L_1$  converts to  $L_2$ , with the crystallisation of  $\alpha$  if the temperature is reduced below  $T_L$ .  $\alpha$  will then start to crystallise from  $L_2$ . A liquid of composition  $c_0$  on cooling to the liquidus temperature  $T_0$  will deposit  $\alpha$ , and its composition will follow the liquidus curve to M, whereupon  $L_1$  will convert to  $L_2$  in the manner previously described.

Delves has shown that the growth of  $\alpha$  from liquid  $L_1$  at the monotectic point can occur at moderate growth rates without giving rise to conditions of constitutional supercooling, since the excess tellurium is rejected at the solid/liquid interface in the form of an additional phase (liquid  $L_2$ ) and is removed by convective rather than diffusive transport. Nevertheless, it is not immediately obvious how to grow from one of the liquids by making use of a thin zone of the other. The LLS TAZC process can be described in the following way. During the growth of  $\alpha$  from liquid of composition  $c_{L1}$ , liquid  $L_2$  of composition  $c_{L2}$  forms. The latter, we believe, will nucleate at the S/ $L_1$  interface. As growth proceeds, this  $L_2$  zone will thicken and a concentration gradient of tellurium will be established across it. If, however, the  $L_2$  zone can be kept thin by some means, say mechanically, then, because the two phase boundaries S/ $L_2$  and  $L_2$ / $L_1$  are in local thermodynamic equilibrium defined by a single liquidus line (that to the right of  $c_{L2}$ ), the process possesses the advantage of other TAZC processes; namely, that of a dramatic reduction in the gradient of constitutional supercooling. Thus, the crystalline  $\alpha$  phase grows from  $L_1$  via diffusion through a thin zone of  $L_2$ . A

driving force for crystallisation is provided by a temperature gradient across the zone as in section 3.1.1 above. (It could in principle also be applied mechanically, as in the Czochralski technique.) This establishes a concentration gradient of tellurium across  $L_2$  which is determined by the slope of the liquidus to the right of  $c_{L2}$ .

### 3.1.3. Vapour-Liquid-Solid (VLS) Processes

Here the charge is a vapour which is just saturated with respect to the crystallising component(s) at the temperature of the liquid/vapour interface, i.e. is in local thermodynamic equilibrium with the liquid at the liquid/vapour interface. As in the other processes involving the application of a temperature gradient, the crystallising phase is at a lower temperature than the charge. The case in which the vapour is supersaturated with respect to the liquid alloy is considered in section 3.4.1 below. Processes equivalent to TAZC processes in which the "thin alloy zone" is a chemical vapour have been reported by Nicoll [13], Kurbatov *et al* [14] and Ziegler [15]. There are many similarities between these processes and TAZC processes.

### 3.2. Pressure Gradient TAZC

The equilibrium liquidus temperature at fixed composition is a function of pressure, hence, in principle, the establishment of a pressure gradient could lead to dissolution and solidification at the two interfaces in an analogous manner to that described above. The motion of a weighted wire through a block of impure ice is an example of this principle.

### 3.3. Electrochemical Potential Gradient

#### TAZC: The Use of an Electric Current and Direct-Current Induced TAZC

In section 3.1 above, zone motion resulted when a concentration gradient was established across an alloy zone as a result of an applied temperature gradient. Pfann, Benson, and Wernick [16] observed the motion of alloy zones along the surface of a germanium bar through which a large direct current was passing. They ascribed the motion to the presence of a temperature gradient across the liquid zone which was generated by the Peltier effect at the solid/liquid interfaces. This interpretation has been critically reviewed by Hurle, Mullin, and Pike [1] and the importance of differential ion migration in the liquid in explaining these effects has been

emphasised. It is clear from fig. 5 that zone motion would also result if a concentration gradient in the liquid were established in an isothermal system. It is possible to establish a concentration gradient if appreciable differential ion migration between the components of the alloy occurs under the influence of a direct electric current. Alloys of the Au-Ge system do show marked ion-migration effects.

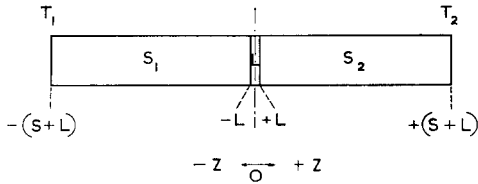


Figure 4 Schematic representation of a TAZC sandwich.

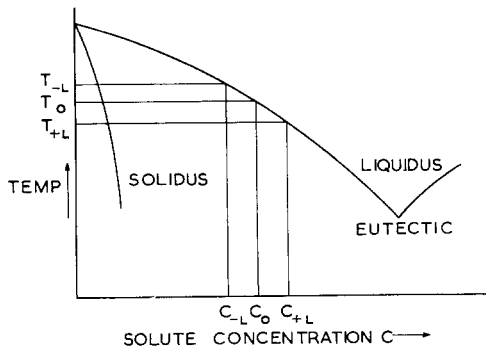


Figure 5 Binary phase diagram showing concentrations and temperatures at phase boundaries in TGZM.

The gold migrates towards the anode. Thus, if a direct current is passed axially through the composite bar shown in fig. 4, gold migrates preferentially towards the positive solid/liquid interface, thereby tending to reduce the liquidus temperature at the positive interface and raise it at the negative interface. As a consequence, germanium dissolves at the positive interface and crystallises out of the liquid at the negative interface in order to maintain solid/liquid equilibrium at the interfaces. The zone therefore moves towards the positive electrode, i.e. in the direction of preferential motion of the gold.

The possibilities of using liquid or vapour phases as the charge should be noted.

### 3.4. Metastable Phase TAZC

It is possible to achieve motion of an alloy zone in an isothermal, isobaric bar through the use of a metastable phase. Consider a situation as

depicted in fig. 4, where  $S_1$  and  $S_2$  are, respectively, stable and metastable phases of a material A, and the zone is a liquid phase containing A and B, where B is virtually insoluble in solid A. The chemical potential of A in the metastable phase  $S_2$  is greater than that of A in the stable phase  $S_1$ ; then if  $S_1$  and  $S_2$  can reach local thermodynamic equilibrium at the  $S_1$ /liquid and the liquid/ $S_2$  phase interfaces respectively, a concentration gradient of A will be established in the liquid zone. A will then diffuse across the zone causing  $S_1$  to grow at the expense of the metastable phase  $S_2$ . More detailed situations in which the metastable phase  $S_2$  is either a solid or a vapour will be considered. The use of a liquid phase  $S_2$  may also be feasible.

#### 3.4.1. SLS Processes

The attainment of a difference in chemical potential at a fixed composition, temperature, and pressure can, in principle, be realised either by having one solid in a highly disordered form (e.g. highly strained) or by arranging that  $S_1$  and  $S_2$  are polymorphs of the same substance. The second case can be reviewed with reference to fig. 6. Here we show the phase diagram for a substance X existing in two polymorphic forms,  $\alpha$  and  $\beta$ , with a transformation temperature  $T_0$ . X is dissolved by Y, but Y is virtually insoluble in solid X. A discontinuity in the slope of the liquidus must exist at  $T_0$ . The  $\beta/\gamma$  and the  $\gamma/\delta$  phase transitions of manganese in the Mn-P system are of this type. The grey ( $\alpha$ ) tin,  $\gamma$ -phase-mercury tin amalgam [17] is an equivalent system.

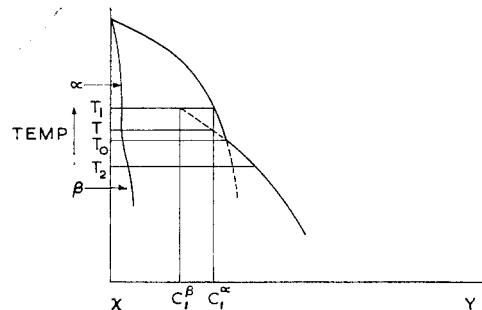


Figure 6 Phase diagram of a binary system X-Y, where solid X undergoes a polymorphic phase transformation at temperature  $T_0$ .

Suppose we wish to grow a single crystal of the  $\alpha$  phase (fig. 6) and have available the low-

temperature form,  $\beta$ . In principle, the  $\alpha$  phase could be grown from the pure melt; however, this may be technologically difficult on account of either a very high melting point, high melting pressure, or the volatility of the substance. We therefore choose to grow it from a solution in  $Y$  at a temperature  $T$ , just above the transformation temperature  $T_0$ . Consider a sandwich structure, as in fig. 4, in which  $S_1$  is the stable phase  $\alpha$ ,  $S_2$  is the unstable  $\beta$  phase (at  $T_1$ ), and the liquid zone has a composition  $c^{\alpha_1}$  at the  $S_1$ /liquid interface. It is assumed that the  $\beta$  phase does not spontaneously transform to  $\alpha$  at  $T_1$  (see below). The liquid is in equilibrium with the  $\alpha$  seed, but by dotting back the  $\beta$  liquidus into the metastable region we see that the liquid is superheated with respect to the  $\beta$  charge. The latter therefore dissolves, endeavouring to attain the composition  $c^{\beta_1}$ . The dissolution of  $\beta$  produces a concentration gradient in the liquid, causing the zone to move in an analogous manner to that described above. Similarly,  $\beta$  could be grown from  $\alpha$  at a temperature  $T_2$ , which is below  $T_0$ .

The  $\alpha$  phase grows by dissolution of  $\beta$  followed by transport across the liquid zone and finally heterogeneous nucleation on the  $\alpha$  phase. Naturally, the directional transformation would not work if the  $\beta$  phase transformed homogeneously into the  $\alpha$  by a solid-state reaction. Such processes are known, but provided the  $\beta$  charge is free from impurities liable to cause heterogeneous nucleation, and provided  $T_1 \approx T_0$ , the activation energy for the desired process involving transport through the liquid zone should be much smaller than for the solid-state reaction.

If we start with the sandwich of  $\alpha$ ,  $\beta$ , and liquid of composition  $c^{\alpha_1}$  as before, but now apply a temperature gradient such that the  $\alpha$ /liquid interface is at  $T_1$  and the  $\beta$ /liquid interface is at some lower temperature  $T$ , the  $\alpha$  phase is in thermodynamic equilibrium with the liquid and the  $\beta$  phase is in pseudo-equilibrium with the same liquid. Thus we may expect no zone motion. We have prevented the growth of the stable  $\alpha$  phase at the expense of the  $\beta$  phase by the application of a temperature gradient.

It is logical that the application of a steeper temperature gradient will cause the reaction to proceed in the opposite direction. In effect, the  $\beta$  phase will grow under conditions in which  $\alpha$  is the thermodynamically stable phase.

### 3.4.2. VLS Processes

A VLS process for single crystal growth has been reported recently by Wagner and Ellis [18]. This can be classified as a metastable-phase TAZC process. Silicon chloride was reduced with hydrogen on a silicon substrate on which were placed dots of gold. Whiskers of silicon grew rapidly on the site of the gold. The gold remained at the top of the whiskers as a liquid Au-Si zone whilst the silicon diffused through the zone and crystallised on the substrate.

Consider fig. 7, the situation in an idealised VLS TAZC process. Vapour  $V_{\alpha\gamma}$ , a volatile compound of  $\alpha$ , together, if necessary, with another gas reacts to form pure  $\alpha$  at the vapour/liquid interface, i.e. a heterogeneous reaction in which the volatile products are removed in the gas phase and are not involved further.  $\alpha$  is soluble in the liquid  $\alpha\beta$  and is transported across the thin liquid zone under the influence of the concentration gradient of  $\alpha$  in the zone.  $\alpha$  crystallises on the solid  $S_\alpha$  at the solid/liquid interface.

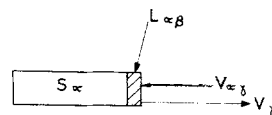


Figure 7 Schematic representation of a VLS process.

If we consider that the vapour reacts to form  $\alpha$  at the liquid/vapour interface with an activity equivalent to a partial vapour pressure of  $\alpha$  of  $\bar{p}$  when the equilibrium vapour pressure of pure  $\alpha$  at the temperature of the process is  $p_0$ , then the driving force for the reaction derives from the fact that  $\bar{p} > p_0$ . Further, since in general elements and compounds can be grown from alloy melts well below their melting points under conditions close to thermodynamic equilibrium, one might expect growth in a VLS process to occur at low supersaturation  $(\bar{p}-p_0)/p_0$  in the gas phase [2].

### 3.4.3. LLS Processes

We refer the reader back to section 3.1.2 for details of the use of two immiscible liquids in TAZC. With reference to fig. 4, we here consider the possibility of having liquid  $L_1$  metastable with respect to the solid – i.e. at a temperature below  $T_M$  the monotectic temperature. Crystallisation would take place by diffusion from  $L_1$  through the thin zone of  $L_2$  to the

solid  $\alpha$ . However, for this to occur, the metastable  $L_1$  must not convert spontaneously to  $L_2$ . This latter requirement appears to demand restrictive and improbable properties of the system.

### 3.5. Combined Processes

It is of course possible to employ two or more driving forces simultaneously. This may be desirable for several reasons:

- (a) To reduce the gradient of constitutional supercooling in metastable-phase processes (see section 4.2.1).
- (b) To achieve stability of the thin alloy zone.
- (c) To control the properties of the crystal, e.g. modulating the steady driving force provided by a temperature gradient with a varying, direct electric current, in order to alter the impurity content of a growing semiconductor crystal.

## 4. Theory

To obtain expressions for the steady velocity of the zone and the gradient of constitutional supercooling at a point in it, in a given TAZC process, we have, in general, to solve the second-order equations of heat and particle transport in the various phases subject to certain boundary conditions. These boundary conditions express: (i) local thermodynamic equilibrium at the phase boundaries; (ii) flow balance across the phase boundaries; and (iii) the imposed driving force(s). In the general case, the transport equations must be derived by the methods of classical irreversible thermodynamics [19]. In the simple case, where there is only one driving force, these reduce simply to Fick's, Fourier's, or Ohm's laws.

We confine ourselves to SLS processes (VLS processes were briefly considered in reference 2). We stress though that there is no essential difficulty in applying the analysis to any TAZC process; the calculation proceeds as illustrated with reference to SLS processes below, but with boundary values appropriate to the particular phase equilibria considered.

### 4.1. The Velocity of a Thin Alloy Zone

The present authors have published a derivation of the velocity of a thin alloy zone moving under the influence of a temperature gradient and an electric current [1]. Account was taken of the Joule, Peltier, Thomson, and ionic-migration effects of the electric current. The published analysis did not include, however, a considera-

tion of the effect of a gradient of chemical potential resulting from the presence of a metastable phase. The extension of the analysis to include this effect is performed in this section; it involves modification of the statements expressing the conditions of thermodynamic equilibrium at the solid/liquid interfaces.

With reference to fig. 4, we consider a long, composite bar formed of two, solid bars ( $S_1$  and  $S_2$ ) of equal length  $S$ , between which is sandwiched a liquid alloy zone of length  $2L$ . The ends of  $S_1$  and  $S_2$  remote from the liquid zone are maintained at temperatures  $T_1$  and  $T_2$  respectively and an axial, direct current of density  $I$  A/cm<sup>2</sup> is passed through the bar. Other assumptions employed are to be found in [1]. The temperature distribution in the liquid alloy zone is given by [1]

$$T_L(Z) = a_L + b_L \exp(-\gamma_L Z) - Q_L Z / \gamma_L \quad (1)$$

where:  $T_L(Z)$  is the temperature in the liquid in the plane  $Z$ ;  $Q_L$  equals  $\rho_L I^2 / K_L$ ;  $\rho_L$  is the electrical resistivity of the liquid alloy;  $K_L$ , the thermal conductivity of the liquid alloy;  $\gamma_L$  equals  $S_L v / K_L$ ;  $S_L$  is the specific heat of the liquid alloy; and  $v$ , the steady velocity of the zone.  $a_L$  and  $b_L$  are complicated algebraic expressions (equations 10a and 10b of [1]) involving  $v$ ,  $I$ ,  $S$ ,  $L$  and the parameters of the solid and liquid phases.

The distribution of solute concentration in the zone  $c(Z)$  is given by [1]

$$c(Z) = \frac{2\eta L \phi \exp(-\eta Z)}{\exp(\eta L) - \exp(-\eta L)} \quad (2)$$

where:  $\eta$  equals  $(v - \Delta\mu E) / D$ ;  $D$  is the diffusion coefficient of the solute in the solvent;  $\Delta\mu$ , the differential ionic mobility of the solute with respect to the solvent in the electric field  $E$  (assumed constant) (Angus *et al* [20], Pfann and Wagner [21]); and  $\phi$ , the average solute concentration in the zone.

$$\phi = \frac{1}{2L} \int_{-L}^{+L} c(Z) dZ$$

In writing (2), we have assumed that the solute is insoluble in the solid.

With reference to fig. 8, the new conditions of thermodynamic equilibrium at the solid/liquid interfaces, which take account of the fact that one of the solid phases is metastable, are:

$$m_1 \{c(-L) - c_\alpha\} = T(-L) - T_\alpha \quad (3)$$

$$m_2\{c(+L) - c_\alpha\} = T(+L) - T_\alpha \quad (4)$$

where

$$m_i = \frac{1}{c_i} \int_{c_\alpha}^{c_i} \left( \frac{dT_i^E}{dc} \right)_c dc \quad (i=1,2)$$

where  $c_1 = c(-L)$  and  $c_2 = c(+L)$ , and  $(dT_i^E/dc)_c$  is the slope of liquidus with respect to solid phase  $i$  at liquid composition  $c$ .  $c_\alpha$  and  $T_\alpha$  are, respectively, the concentration and temperature corresponding to the phase transformation.

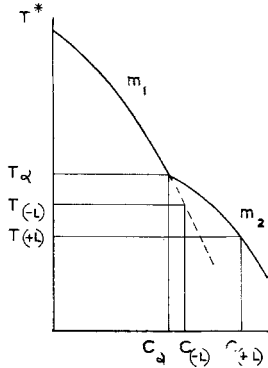


Figure 8 Phase diagram of a binary system with polymorphic phase transformation.

In the absence of a metastable phase, we take  $T^*$  (the melting point of  $S_1$  and  $S_2$ ) as our reference temperature in (3) and (4). In this case, putting  $m_1 = m_2$ ,  $c_\alpha = 0$ , and  $T_\alpha = T^*$ , we obtain the equations 15 and 16 in [1].

Substituting (1) and (2) into (3) and (4), we obtain a pair of simultaneous equations in  $v$  and  $\phi$ . A zone of length  $2L$  will move with a steady velocity  $v$  only if  $\phi$  is chosen so as to satisfy simultaneously this pair of equations.

Adding (3) and (4), we obtain the following equation for  $\phi$ :

$$2\eta L\phi \frac{[m_1 \exp(\eta L) + m_2 \exp(-\eta L)]}{[\exp(\eta L) - \exp(-\eta L)]} - (m_1 + m_2)c_\alpha - 2(a_L - T_\alpha) - b_L[\exp(\gamma_L L) + \exp(-\gamma_L L)] = 0 \quad (5)$$

Subtracting (3) from (4) we obtain

$$\frac{2\eta L\phi}{\exp(\eta L) - \exp(-\eta L)} [m_1 \exp(\eta L) - m_2 \exp(-\eta L)] - (m_1 - m_2)c_\alpha - b_L[\exp(\gamma_L L) - \exp(-\gamma_L L)] - 2Q_L L/\gamma_L = 0 \quad (6)$$

Expanding (5) and (6) to first power in  $L$  and the Thomson coefficient of the solid ( $\tau_S$ ) - which

$$v = \frac{\frac{K_S(T_1 - T_2)}{2S} - PI + \frac{\Delta\mu I\rho_L K_L}{D} m\phi - \frac{\rho_S I^3 S^2 \tau_S}{6K_S} - \frac{\Delta m}{L} K_L(\phi - c_\alpha)}{\frac{K_L}{D} m\phi - H - \frac{S_S \rho_S I^2 S^2}{6K_S}} \quad (7)$$

is contained in  $a_L$  and  $b_L$  - we obtain, after lengthy manipulation, the expression for  $v$  (see equation 7) where:  $K_S$  is the thermal conductivity of the solid phase;  $P$ , the Peltier coefficient at the solid/liquid interfaces;  $\rho_S$ , the electrical resistivity of the solid phase;  $H$ , the latent heat of fusion of solid phases;  $m$  equals  $(m_1 + m_2)/2$ ; and  $\Delta m$  equals  $(m_1 - m_2)/2$ .

Equation 7 contains an implicit dependence of  $\phi$  on  $L$ . The equation differs from the result obtained in [1] only by the addition of the last term in the numerator which represents the contribution to the velocity made by the isothermal, chemical-potential difference between the two solid phases.

For a discussion of the physical significance of the various terms the reader is referred to [1]. However, we discuss below two further special cases in which there is a metastable phase.

Case 1

$$I = 0, m\phi \gg \frac{D}{K_L} \left( H + \frac{\rho_S I^2 S^2 S_S}{6K_S} \right), T_1 = T_2$$

$$v = - \frac{\Delta m (\phi - c_\alpha) D}{L m \phi} \quad (8)$$

This is the steady velocity due to the higher chemical potential possessed by the metastable phase. Notice that  $v$  is proportional to  $(m_1 - m_2)(\phi - c_\alpha)$  - which is a measure of the difference in chemical potential between the two solids - and inversely proportional to the length of the zone. (The expression is only valid, though, for small  $L$  and  $v$ .)

Case 2

$$I = 0, m\phi \gg \frac{D}{K_L} \left( H + \frac{\rho_S I^2 S^2 S_S}{6K_S} \right)$$

$$v = \frac{\frac{K_S(T_1 - T_2)}{2S} - \frac{\Delta m (\phi - c_\alpha)}{L}}{m\phi/D} \quad (9)$$



Equation 9 shows that the driving force due to the gradient of chemical potential is over-riden by the temperature gradient if

$$\frac{K_S (T_1 - T_2)}{K_L 2S} > \frac{\Delta m (\phi - c_\alpha)}{L} \quad (10)$$

Under these circumstances, the thermodynamically "unstable" phase grows at the expense of the stable phase. The inequality (10) will be satisfied for some sufficiently large temperature gradient and some, not too small, values of  $L$ .

The implications of the assumption that the solid/liquid interfaces are in local equilibrium (equations 3 and 4) require elaboration. The reader might argue that if the interfaces are in thermodynamic equilibrium then by definition no reaction can take place, i.e. no zone motion can occur. Indeed, some, very small supercooling must exist at the freezing interface and superheating at the melting interface. However, the assumption is that the velocity of the zone is limited not by the activated processes occurring at the interfaces but rather by diffusion across the liquid alloy zone. Under such circumstances, it is quite valid to ignore the very small displacements from equilibrium which exist at the interfaces, since they in no way control the reaction. The general analysis, taking into account the activated processes at the interfaces, has not yet been developed, though special cases have been considered by Tiller [22]. In some systems, zone velocity will be limited by diffusion; in others, by either the rate of dissolution or crystallisation. The above theory is valid only for diffusion-controlled systems. Experimental evidence has been presented by Mlavsky and Weinstein [23] and Griffiths and Mlavsky [24] which strongly suggests that, in the system GaAs-Ga and SiC-Cr, diffusion is the rate-limiting process in the movement of zones by a temperature gradient. On the other hand, Wernick [25] found a strong dependence of zone velocity on temperature in a germanium alloy system, which indicates that some process other than diffusion is rate limiting. Van Lent [26] concluded that dissolution was the rate-limiting process in the growth of grey tin from

mercury-white tin alloys, but the present authors feel that this was not conclusively proved.

#### 4.2. Constitutional Supercooling

It was stated earlier that one of the advantages of TAZC over conventional flux-growth techniques was that the gradient of constitutional supercooling at a given zone velocity was smaller with the thinner zone. In this section, we derive analytical expressions for the gradient of constitutional supercooling which illustrate this point.

We confine ourselves to systems for which  $\Delta\mu = 0$ , since, as we shall see in section 4.3, the concept of constitutional supercooling is of little value when there is ionic transport.

The constitutional supercooling,  $S_i(Z)$ , with respect to the solid  $i$  in the plane  $Z$ , is given by:

$$S_i(Z) = m_i [c(Z) - C_\alpha] - [T_L(Z) - T_\alpha] \quad (11)$$

Thus, differentiating (11)

$$\frac{dS_i(Z)}{dZ} = m_i \frac{dc(Z)}{dZ} - \frac{dT_L(Z)}{dZ} \quad (12)$$

Substitution of (1) and (2) into (12), putting  $\Delta\mu = 0$ , yields

$$\frac{dS_i(Z)}{dZ} = - \frac{2v^2 L m_i \phi}{D^2} \frac{\exp(-\eta'Z)}{\exp(\eta'L) - \exp(-\eta'L)} + \gamma_L b_L \exp(-\gamma_L Z) + Q_L / \gamma_L \quad (13)$$

where  $\eta' = v/D$

Equation 13 can be put into a more useful form using (5) and (6) (see equation 14).

##### 4.2.1. The Thin Zone

We use this term to apply to zones for which  $\eta'L \ll 1$  and  $\gamma_L L \ll 1$ .

Equation 14 can then be expanded in the form

$$\frac{dS_i(Z)}{dZ} = (m - m_i) \phi \eta' + \frac{\Delta m (\phi - c_\alpha)}{L} + (m_i \phi \eta'^2 - b_L \gamma_L^2) Z \quad (15)$$

The first two terms in (15) arise from the presence of a chemical-potential-gradient effect. When  $m_1 = m_2$ , (15) reduces approximately to

$$\frac{dS_i(Z)}{dZ} = \frac{\eta' \phi}{[\exp(\eta'L) - \exp(-\eta'L)]} \left\{ m_1 \exp(\eta'L) - m_2 \exp(-\eta'L) - 2\eta' m_i L \exp(-\eta'Z) \right\} - \Delta m c_\alpha / L + b_L \left\{ \gamma_L \exp(-\gamma_L Z) - \frac{[\exp(\gamma_L L) - \exp(-\gamma_L L)]}{2L} \right\} \quad (14)$$

$$\frac{dS(Z)}{dZ} = \frac{m\phi v^2}{D^2} Z \quad (16)$$

The gradient of supercooling at the freezing interface is thus

$$\left(\frac{dS}{dn}\right)_{fi} = -\frac{m\phi v^2 L}{D^2} (> 0 \text{ since } m < 0) \quad (16a)$$

where  $n$  = normal into the liquid at the freezing solid/liquid interface. Note that the gradient of supercooling is proportional to  $L$  and  $v^2$ . For  $m\phi = -500^\circ \text{C}$ ,  $v = 10^{-4} \text{cm/sec}$ ,  $D = 10^{-4} \text{cm}^2/\text{sec}$ , and  $L = 10^{-3} \text{cm}$

$$\left(\frac{dS}{dn}\right)_{fi} = 0.5^\circ \text{C/cm}$$

This figure is well below the critical gradient of constitutional supercooling which the (111) surface of germanium will withstand [27].

When the chemical-potential gradient resulting from the presence of the metastable phase is the driving force for zone motion, the first two terms in (15) dominate and

$$\frac{dS_i(Z)}{dZ} = \frac{(m - m_i)\phi v}{D} + \frac{\Delta m(\phi - c_a)}{L} \quad (17)$$

Using (8) we obtain the following alternative forms of (17)

$$\left(\frac{dS_i}{dn}\right)_{fi} = -\frac{m_i\phi |v|}{D} \quad (18)$$

$$= \frac{m_i |\Delta m(\phi - c_a)|}{Lm} \quad (19)$$

(Notice that the gradient is independent of  $Z$  for small  $L$  and proportional to  $v$  or to  $1/L$  which is equivalent.)

Inserting the above values of the parameters in (18)

$$\left(\frac{dS_i}{dn}\right)_{fi} = 500^\circ \text{C/cm}$$

we see that the gradient of supercooling is *not* small in this case; in fact, it increases with decreasing zone length. This result provides a probable explanation for the entrapment of mercury inclusions in grey tin found by Van Lent [26].

However, if we oppose this "metastable-phase" driving force by some other thermodynamic driving force, say a temperature gradient, we see that there are some conditions under which this supercooling disappears.

Inserting (9) into (17), we obtain an extended form of (18) for the special case 2 above

$$\frac{dS_i(Z)}{dZ} = -\frac{m_i\phi v}{D} + \frac{K_S(T_1 - T_2)}{K_L 2S} \quad (20)$$

The significance of (20) can be understood with reference to figs. 9 and 10. Fig. 9 shows the isothermal situation in which the liquid is supercooled with respect to the freezing solid  $S_1$  with gradient

$$\frac{dS_1}{dZ} = -\frac{m_1\phi v}{D}$$

and superheating with respect to  $S_2$  with gradient

$$\frac{dS_2}{dZ} = -\frac{m_2\phi v}{D}$$

Fig. 10 shows the case in which a thermal gradient is applied to reduce  $v$  to zero: i.e. from (9)

$$\frac{K_S(T_1 - T_2)}{K_L 2S} = \frac{\Delta m(\phi - c_a)}{L}$$

With respect to  $S_1$ , the liquid is supercooled with gradient

$$\frac{dS_1}{dZ} = \frac{K_S(T_1 - T_2)}{K_L 2S}$$

and superheated with respect to  $S_2$  with the same gradient. If now the temperature gradient is further increased, then  $S_2$  freezes and  $S_1$  melts and the whole melt is superheated (rather than supercooled) with respect to the freezing interface.

The gradient of constitutional *superheating* is then given by (20). This is shown schematically in fig. 11. Imagine now that we go on increasing the temperature gradient until this greatly overrides the chemical-potential-gradient effect.  $v$  will then be given approximately by

$$v = \frac{K_S D (T_1 - T_2)}{K_L m\phi 2S}$$

and the right-hand side of (20) becomes zero. (However, remember that in deriving (20), the last term in (15) was omitted.)

Thus, it seems, the best way to grow grey tin from white tin would be in the white-tin stable region (i.e. above  $13^\circ \text{C}$ ) using a steep temperature gradient – a curious result.

#### 4.2.2. The "Thick" Zone

We use this term to apply to zones for which

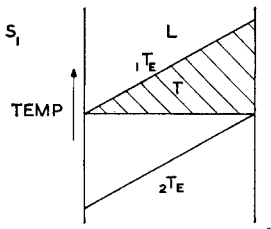


Figure 9 Isothermal, thin alloy zone with phase  $S_1$  crystallising. The liquid is constitutionally supercooled with respect to  $S_1$  (hatched area) but superheated with respect to  $S_2$ .

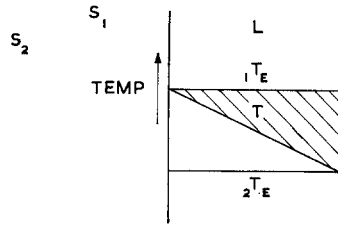


Figure 10 Thin alloy zone with metastable phase ( $S_2$ ) and temperature gradient such that solute concentration in the zone is uniform (i.e. no zone motion occurs). The liquid is constitutionally supercooled with respect to  $S_1$  (hatched area).

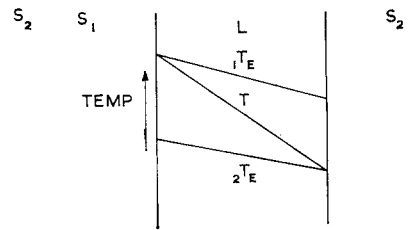


Figure 11 Thin alloy zone with metastable phase ( $S_2$ ) and temperature gradient such that  $S_2$  crystallises and  $S_1$  dissolves. The liquid is superheated with respect to the crystallising phase.

$\eta'L \gg 1$  and  $\gamma_L L \ll 1$ . Here  $L$  is in general so large (order of centimetres) that the gradient of chemical potential resulting from the use of a metastable phase is negligible. We therefore set  $m_1 = m_2$  and  $c_\alpha = 0$ . From (14)

$$\frac{dS(Z)}{dZ} = m\phi\eta' \left\{ 1 - \left[ \frac{2\eta'L \exp(-\eta'Z)}{\exp(\eta'L) - \exp(-\eta'L)} \right] - b_L \gamma^2 L Z \right\} \quad (21)$$

The last term is again negligible. In the limit  $\eta'L \gg 1$ , the gradient of constitutional supercooling at the freezing interface is, from (21),

$$\left( \frac{dS}{dn} \right)_{fi} = - \frac{2m\phi\eta^2 L}{D^2} \quad (22)$$

This result will be compared with the other cases below.

#### 4.2.3. Interface Stability

(i) *General considerations* The development of a cellular structure and the consequent micro-segregation of solute, in the presence of a positive gradient of constitutional supercooling, has already been mentioned. The correlation between the presence of constitutional supercooling and the instability of a planar interface has been investigated theoretically by Mullins and Sekerka [28]. Except in systems with a high, solid/liquid, interfacial energy, the correlation can be stated as follows.

When a perturbation in the shape of a non-habit freezing solid/liquid interface results only in the redistribution of solute by diffusion, then this instability can be correlated with the onset of a positive gradient of constitutional super-

cooling in the melt. Now, in general, all the transport coefficients will have different values in the two phases and hence all the flow vectors will be modified by the change in the interface morphology. However, the redistribution of the thermal flow as a result of the formation of a cellular morphology (with cell dimensions typically  $10^{-2}$  cm) is small and can be neglected on account of the high thermal diffusivity compared to the solute diffusivity (the latter is typically  $10^{-4}$  to  $10^{-5}$  cm<sup>2</sup>/sec; the former, for germanium, is  $\sim 10^{-1}$  cm<sup>2</sup>/sec). The electrical resistivities of solid semiconductors are generally much greater than those of alloy melts, and hence, in such a system, a marked redistribution of a current through the solid/liquid interface takes place if a cellular structure forms. Again, because of the high thermal diffusivity, the redistribution of the thermal sources of the current can probably be neglected. However, the redistribution of the ionic current must be taken into account. Thus, in the presence of ionic migration, the concept of constitutional supercooling alone is of no value in predicting the condition for the stability of a planar solid/liquid interface. A perturbation calculation which would predict the stability conditions would be extremely complicated, and has not yet been performed. We can therefore only give a qualitative account of the factors affecting interface stability in the presence of ionic currents.

(ii) *The effect of an electric current* We consider two classes of systems for which  $\rho_S \geq \rho_L$  respectively. These are illustrated in figs. 12a and b.  $\rho_S$  and  $\rho_L$  are the electrical resistivities of the solid and liquid phases respectively. If a

sinusoidal perturbation in the shape of the interface occurs, the current flow lines will be redistributed as indicated in the figure. For a solid semiconductor/alloy melt where  $\rho_s > \rho_L$ , the current density will increase in the cell boundaries. In a solid-metal/liquid-metal alloy system for which  $\rho_s < \rho_L$ , the current will be concentrated at the cell peaks.

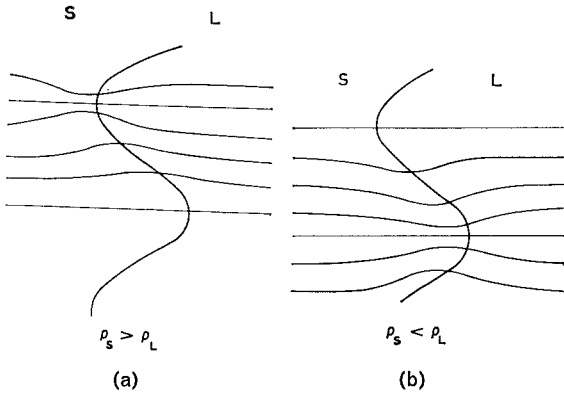


Figure 12 Schematic representation of the current distribution in the vicinity of a cellular interface: (a)  $\rho_s > \rho_L$ ; (b)  $\rho_s < \rho_L$  ( $\rho =$  resistivity).

If the ionic current redistribution is such as to carry relatively more solute into the cell boundaries, the cellular morphology will tend to be stabilised, if less, then the interface will tend to relax back to a plane. Thus it is possible, in general, either for a cellular morphology to exist in the absence of constitutional supercooling or for a planar interface to be stabilised in the presence of constitutional supercooling. The conditions are summarised for the two cases  $\rho_s \geq \rho_L$  in table II. Also in the table are the thermal effects of the current, but as indicated above these are thought to be less important.

TABLE II Stability of a planar solid/liquid interface through which a direct current is passed (*u* = unstable and *s* = stable).

Electrical effect	Sign of effect	Resistivity ratio	
		$\rho_s > \rho_L$	$\rho_s < \rho_L$
Peltier	Interface heated	u	s
	Interface cooled	s	u
Joule	—	u	s
Ionic Migration	Solute to interface	u	s
	Solute from interface	s	u

4.2.4. Discussion and Summary

The gradient of constitutional supercooling at

the interface of a crystal growing from a stirred melt, as in the Czochralski method [7], is

$$\left(\frac{dS}{dn}\right)_{fi} = \frac{-mv\phi(1-k)}{D\left\{k + (1-k)\exp\left(\frac{-v\delta}{D}\right)\right\}} - \left(\frac{dT_L}{dn}\right)_{fi} \tag{23}$$

where  $\phi$  is here the concentration in the bulk of the melt,  $k$  is the segregation coefficient,  $\delta$  is the boundary-layer thickness [29] (where  $\delta \propto \omega^{-\frac{1}{2}}$  in the Czochralski method:  $\omega$  is the angular velocity of the crystal). Under conditions of very good stirring for which  $v\delta/D \ll 1$  and with  $k = 0$ , (23) reduces to

$$\left(\frac{dS}{dn}\right)_{fi} = -\frac{m\phi v}{D} - \left(\frac{dT_L}{dn}\right)_{fi} \tag{24}$$

Table III summarises the approximate expressions for  $(dS/dn)_{fi}$  for the various crystal-growing processes discussed.

From table III we see the great advantage of TAZC (without the use of a metastable phase). At fixed velocity, the gradient of constitutional supercooling in a thick zone is greater than that in a thin zone by a factor of

$$\frac{2 \times (\text{length of "thick" zone})}{(\text{length of "thin" zone})}$$

In Trumbore's thermal-gradient method [4], the zone length is typically  $\sim 5$  cm. Thin-zone experiments are carried out with typical zone lengths of  $5 \times 10^{-3}$  cm. The ratio of the gradients of constitutional-supercooling thick zone to thin is then  $2 \times 10^3$ . Alternatively, if some critical gradient of constitutional supercooling must not be exceeded, if liquid droplet entrapment is to be avoided, then the velocity of the thick zone must be roughly 50 times smaller than that of the thin zone. This accounts for the experimental fact that maximum velocities obtainable by Trumbore [4] are much lower than those of Mlavsky and his coworkers [23, 24].

It is interesting to note that the gradient of supercooling at fixed velocity is greater with the thick-zone techniques than with the Czochralski technique. The problem with the latter technique lies in achieving a sufficiently uniform motion of the pull rod and avoidance of thermal fluctuations, although growth rates will still be much lower than are obtainable by TAZC.

It can readily be shown that the value of  $(dS/dn)_{fi}$  for a vapour-phase TAZC process is

TABLE III

Technique	Condition satisfied	$\left(\frac{dS}{dn}\right)_{fi}$	Comments
(a) TGZM and/or dc induced TAZC	$\frac{vL}{D} \ll 1$	$-\frac{m_i\phi v^2 L}{D^2}$	Effects of ionic migration excluded
(b) Metastable phase TAZC	$\frac{vL}{D} \ll 1$	$-\frac{m_i\phi v}{D}$	
(c) Thermal gradient technique	$\frac{vL}{D} \gg 1$	$-\frac{2m_i\phi v^2 L}{D^2}$	
(d) Czochralski	$\frac{v\delta}{D} \approx 1$	$-\frac{m_i\phi v}{D} - \left(\frac{dT_L}{dn}\right)_{fi}$	Valid only under conditions of good stirring

the same as that for the polymorphic transformation, namely, that given in row b in table III.

## 5. Some Applications

### 5.1. Production of Homogeneous Single Crystals

The TAZC technique could in principle be applied to a large number of materials in order to produce homogeneous single crystals. The successful applications, however, appear to be confined to semiconducting materials. The main experimental problem in applying the technique involves maintaining a stable lamellar geometry for the liquid zone. One cause of zone instability results from the motion of liquid preferentially into grain boundaries: another cause of zone instability is constitutional supercooling occurring with thick zones [30]. Grain boundaries in Group IV or Group III-V semiconductors can cause zone instability. It is essential with these materials to achieve complete wetting of the seed crystal and this may require exacting experimental techniques [23, 24, 31]. Nevertheless, the wetting is probably no greater problem than that of obtaining a sufficiently clean substrate on which to obtain high-quality epitaxial growth.

The principal advantage of TAZC techniques over other solution-growth techniques is that of the dramatic reduction in the quantity  $(dS/dn)_{fi}$ . This advantage, however, is principally confined to processes not involving the use of a metastable phase. For convenience then, we shall divide our discussion into processes (a) not involving and (b) involving a metastable phase.

#### 5.1.1. Processes Not Involving a Metastable Phase

(i) *TGZM processes* Pfann [11] in his book on zone melting has reviewed the original TGZM

studies that were made on germanium and silicon using laminar alloy zones. More recently, workers at Tyco Laboratories have carried out more systematic studies on GaAs,  $\alpha$ -SiC and GaAs/GaP heterojunctions [23, 24, 31, 32] using this basic technique, but referring to it as the travelling-solvent technique.

(ii) *Direct-current induced TAZC* The limitation on the length of crystal which can be obtained by the above method can, in principle, be largely overcome by the use of dc induced TAZC. The method is, however, limited to materials which have appreciable conductivity at the operating temperature.

We have performed experiments in which Au-Ge liquid alloy zones have been passed through germanium bars using a dc electric field. The experimental arrangement used is shown schematically in fig. 13. Because a high-current lead has to be attached to the top specimen, it cannot readily be "floated" on the liquid zone as in temperature-gradient zone melting. To maintain the correct thickness of the liquid alloy zone, a thin mica washer is used to surround the alloy zone and to space apart the two germanium bars.

Experimentally, a thin disc of gold is placed within the mica washer and the sandwich assembled. The specimen is then heated in vacuo by means of the rf coil and graphite susceptor to the operating temperature. The gold alloys with germanium to form the liquid alloy zone. When equilibrium has been reached, a dc current is applied axially through the bar from a low-voltage constant-current source. The zone moves along the bar towards the positive electrode owing to the effects on ionic migration. These oppose and override the temperature gradient produced by the Peltier effect. At  $\sim 500^\circ\text{C}$ , a zone velocity of 1 mm/h was obtained with a current density of only 10 A/cm<sup>2</sup>.

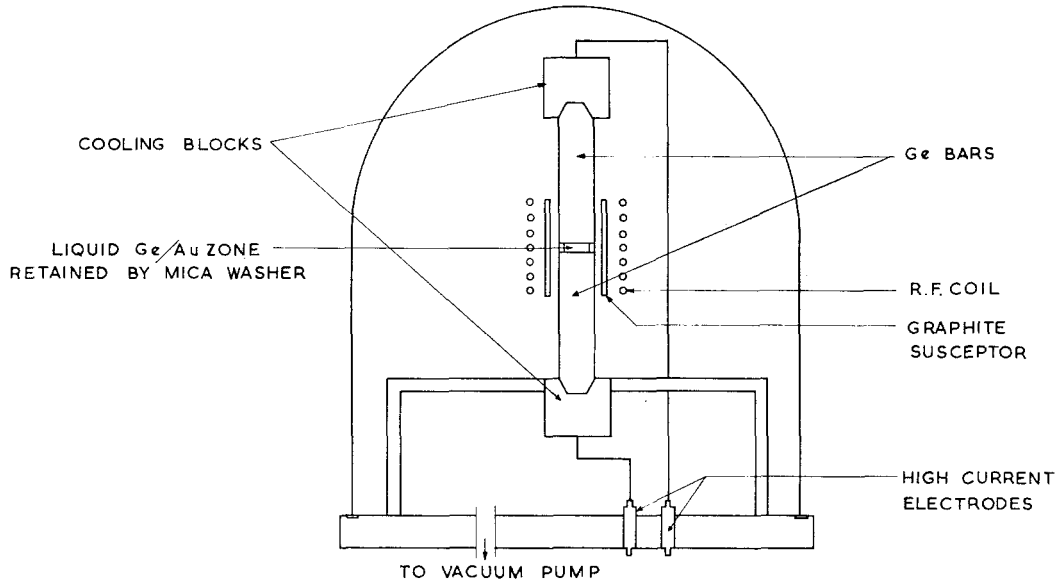


Figure 13 Schematic representation of the apparatus used for dc induced TAZC.

Considerable difficulty has been experienced in maintaining the lamellar form of the zone. This is in fact due to the difficulty in achieving uniform wetting in the presence of the mica washer. If the gold disc is too thick in relation to the thickness of the mica, then, on alloying, molten alloy is exuded out; if too thin, a void is left leading to incomplete wetting.

However, several successful runs have been performed in which single-crystal growth onto the seed crystal has been achieved. Fig. 14 is a micrograph showing the result of a successful run. The problems are made more severe by the large difference in electrical resistivity between solid and liquid phases. The technique should be much more readily applicable to the growth of metal single crystals from alloy melts, where the difference in resistivity between the two phases is only about 2.

It may be that the most important application of TGZM and dc induced TAZC has yet to be realised; namely, its use to grow single crystals of solid solutions (e.g. Ge-Si or InAs-InSb alloys) which cannot readily be grown in any other way. In this case, the charge would have to be cast material of the required average composition and the zone temperature adjusted such that the composition of the crystallising material was equal to that of the dissolving material. This latter requirement ensures that the composition of the zone, and hence its length, does not change as growth proceeds.

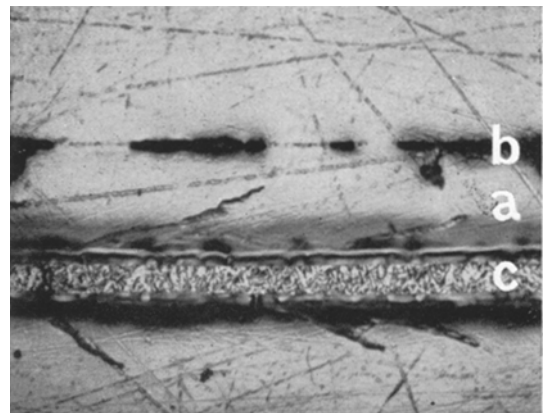


Figure 14 Direct-current induced TAZC. Photomicrograph shows: (a) region of germanium single-crystal growth from a Au-Ge alloy; (b) start of growth; (c) end of growth showing etched Au-Ge eutectic structure.

Another possibility is the use of a direct current to modulate the concentration gradients of solute species in a thin alloy zone in order to produce sharp, planar, alloyed junctions.

#### 5.1.2. Metastable-Phase Processes

The VLS process is potentially the most important TAZC technique in this category. The original experimental work which established this concept was carried out by Wagner and Ellis [18] who studied the effect of various metals on the formation of whiskers [33]. One

advantage in the use of a vapour phase is that the charge material can be generated by a chemical reaction, the unwanted reaction products being removed by diffusion in the gas phase.

The work of Wagner and Ellis [18] on silicon showed that the VLS mechanism was operating in the growth of silicon whiskers from small globules (up to  $\sim 1$  mm diameter) of Au-Si alloy. Whiskers could also be produced if the gold was replaced by small amounts of platinum, silver, copper, or nickel. Small globules of alloy, Cu-Zn in the case of GaP [34], and platinum, palladium, gallium, or gold in the case of GaAs [35], have also been shown to be capable of giving rise to VLS whisker growth.

However, attempts to employ the VLS mechanism to obtain growth normal to an extended, flat plane have encountered a similar difficulty to that found in TGZM and dc induced TAZC, i.e. the difficulty of maintaining a thin, uniform, liquid alloy layer.

Filby and Nielsen [36] found that 1 to 15  $\mu\text{m}$  thick layers of gold, copper, tin, or indium formed alloy layers on heating on a silicon surface and then tended to break up into globules. Nevertheless, by supplying the alloy layers with silicon vapour sublimed from a hot silicon source, epitaxial growth although not of a high quality was achieved by the VLS mechanism. In the case of indium zones, growth was achieved at a temperature as low as 300° C.

James and Lewis [37] found that, contrary to the experience of Filby and Nielsen [36], at temperatures above 1000° C Au-Si alloys did spread out across the silicon slice. However, whilst Filby and Nielsen used evaporated silicon, James and Lewis used  $\text{SiCl}_4 + \text{H}_2$ . It is understandable that the presence of HCl in the latter experiments could aid the wetting of the Au-Si alloys. James also showed that epitaxial growth occurred by the VLS mechanism in his experiments, but the quality of the epitaxial layers did not compare with that achievable by conventional vapour-solid processes.

Related studies using an ultra-thin alloy zone (UTAZC technique) formed from metal films ( $\sim 3000$  Å of Au, Au-Al, or Ag) have been the subject of an investigation by Filby and Nielsen [38]. This technique did result in the growth of single-crystal areas of silicon, but it is not yet clear from these experiments and related ones [39, 40] whether the ultra-thin zone acts as a diffusion medium for the silicon, alters the nucleation

kinetics at the growth interface, or functions in some, as-yet-undefined manner. It is clear, however, that it does show promise for obtaining single-crystal epitaxial films of silicon or a variety of substrates.

The temperature distribution is an important aspect of VLS techniques [36, 37]. Specifically, a positive temperature gradient in the alloy zone ahead of the solid/liquid interface is required. Such a temperature gradient provides a second driving force for the zone motion and also serves to reduce the gradient of constitutional supercooling at fixed velocity. It is conceivable that the likelihood of nucleation at the liquid/vapour interface could also be reduced as a consequence of the increased solubility of the material at that interface.

The SLS principle can be identified in the work of Van Lent [26] on the transformation of mercury/white tin amalgams to grey tin and in the General Electric process [41] for the production of synthetic diamonds. In the latter, metal (for example iron or nickel) and graphite are raised to a high temperature and pressure which lie (i) in the diamond-stable region of the carbon  $p/T$  diagram and (ii) above the metal/carbon eutectic. Typical values are 1400° C and 60 kbars. Diamond nucleation occurs and growth on the nucleated diamonds proceeds at the expense of the graphite via a thin liquid carbon/metal film. The function of the liquid film is thought, by workers at General Electric, to be catalytic [41], but by Giardini and Tydings [42] to be a transport medium.

Van Lent prepared  $\gamma$ -phase alloys of white ( $\beta$ ) tin containing a few per cent of mercury in the form of foil and held them at temperatures of  $-10$  to  $-20$ ° C. The grey ( $\alpha$ ) tin phase was observed to nucleate and grow as a single crystal at rates in the range  $10^{-6}$  to  $10^{-5}$  cm/sec. Very little adhesion between  $\alpha$  and  $\gamma$  phases existed during growth; in fact they were separated by a very thin layer of liquid mercury-rich alloy. The mercury rejected by the growth of the  $\alpha$  phase was found to be removed by diffusion through the  $\gamma$  phase. The grey tin/liquid interface had a faceted (cellular) form and some inclusions of mercury were found in the crystals. It is highly likely that this was the result of the constitutional supercooling which exists in such an isothermal metastable-phase process (section 4.2.1). However, this implies a diffusion-limited reaction, whereas Van Lent concluded that the process was controlled by the dissolution of the  $\gamma$  phase.

The large volume change on transition of grey to white tin (~20%) prevents the growth of strain-free crystals of grey tin by solid-state transformation. The use of a thin, liquid alloy layer to separate the two phases largely overcomes this problem. By employing the lamellar TAZC geometry, using an  $\alpha$ -phase, oriented seed-crystal and additionally employing a temperature gradient as discussed in section 4.2.1, it may be possible to grow fairly large, grey-tin crystals free from strain and mercury inclusions.

The growth of CdS [43, 44], which was brought about by heating CdS on which had been evaporated a thin, metal film (Pb, In, Al, Bi, Zn or ZnS), could also be an example of a metastable-phase TAZC process, although the role of the metal in forming a liquid alloy would need to be definitely established. A number of materials which undergo solid-state recrystallisation [45] are worthy of investigation in the light of a TAZC mechanism, since impurities which could form liquid alloy phases appear to play an important role in the process.

The LLS principle has been demonstrated by Delves [12] in the Hg-Te system; its application to the growth of Ge-Si alloys is the subject of current research. Its application must be fairly limited; not many systems show liquid immiscibility. However, we would note that (i) the elements tellurium, lead, and bismuth form immiscible liquids with silicon and possibly also with some Group III-V compounds and (ii) a whole range of ionic materials show liquid immiscibility when in solution in excess concentrations of the metal ion (e.g.  $\text{CaF}_2/\text{Ca}$ ).

## 5.2. Production of Composite Structures

The motion of "wire" and "dot" zones by TGZM to produce a variety of semiconductor device structures has been extensively considered by Pfann in his book [11] and in his original patent [10]. These range from simple p-n structures to complicated p-n-i-p devices having multiple elements. The reader is referred to the above references for further detail.

We would only remark that, because of the problems of achieving intimate thermal contact between a block of semiconductor and a heat source or sink, it is not always easy to achieve a purely axial temperature gradient in the desired direction. However, because of the large difference in electrical resistivities of semiconductors and liquid metal alloys, a disadvantage with a lamellar zone, as noted above, an electric current

is channelled in the liquid alloy and in doped regrown material. Thus dc induced TAZC could be used instead of TGZM to produce the device structures envisaged by Pfann and should be capable of much more precise control over the shape of the regrown areas.

The use of VLS techniques to obtain preferential epitaxial deposition of silicon on areas which are covered with a thin, metal film (by evaporation through a mask for example) should be possible.

## Acknowledgements

The authors are indebted to their colleagues for numerous discussions and for results of their experimental work, particularly W. Bardsley, R. Delves, B. Cockayne, J. Filby, S. Nielsen, G. J. Rich, D. Robertson, and to W. G. Pfann. The experimental assistance of Mrs J. Harp is gratefully acknowledged.

## References

1. D. T. J. HURLE, J. B. MULLIN, and E. R. PIKE, *Phil. Mag.* **9** (1964) 423.
2. *Idem*, *Solid State Comm.* **2** (1964) 197 and 201.
3. R. A. LAUDISE, "The Art and Science of Growing Crystals" (John Wiley, New York, 1963), p. 252.
4. F. A. TRUMBORE, E. M. PORBANSKY, and A. A. TARTAGLIA, *J. Phys. Chem. Solids* **11** (1959) 239.
5. R. A. LAUDISE, reference 3, p. 261.
6. J. W. NIELSEN, R. C. LINARES, and S. E. KOONCE, *J. Amer. Ceram. Soc.* **45** (1962) 12.
7. D. T. J. HURLE, *Solid State Electron.* **3** (1961) 37.
8. W. BARDSLEY, J. S. BOULTON, and D. T. J. HURLE, *ibid* **5** (1962) 395.
9. W. G. PFANN, *Trans. AIME* **203** (1955) 961.
10. *Idem*, US Patent No. 2,813,048, Nov. 12th (1957).
11. *Idem*, "Zone Melting" (John Wiley, New York, 1958).
12. R. T. DELVES, *Brit. J. Appl. Phys.* **16** (1965) 343.
13. F. H. NICOLL, *J. Electrochem. Soc.* **110** (1963) 1165.
14. B. S. KURBATOV, E. V. RAKOVA, and G. A. KUROV, *Kristallografiya* **10** (1965) 756.
15. G. ZIEGLER, *Solid State Electron.* **6** (1963) 680.
16. W. G. PFANN, K. E. BENSON, and J. H. WERNICK, *J. Electron. Control.* **2** (1957) 597.
17. P. H. VAN LENT, *Acta. Met.* **9** (1961) 125.
18. R. S. WAGNER and W. C. ELLIS, *Appl. Phys. Letters* **4** (1964) 89.
19. D. T. J. HURLE, J. B. MULLIN, and E. R. PIKE, *J. Chem. Phys.* **42** (1965) 1651; **43** (1965) 3420.
20. J. ANGUS, D. V. RAGONE, and E. E. HUCKE, *Met. Soc. Conferences* **8** (1961) 833.
21. W. G. PFANN and R. S. WAGNER, *Trans. AIME* **224** (1962) 1139.
22. W. A. TILLER, *J. Appl. Phys.* **34** (1963) 2763.



23. A. I. MLAVSKY and M. WEINSTEIN, *ibid*, 2885.
24. L. B. GRIFFITHS and A. I. MLAVSKY, *J. Electrochem. Soc.* **111** (1964) 805.
25. J. H. WERNICK, *Trans. AIME* **221** (1957) 1169.
26. P. H. VAN LENT, *Acta Met.* **10** (1962) 1089.
27. W. BARDSLEY, J. M. CALLAN, H. A. CHEDZEY, and D. T. J. HURLE, *Solid State Electron.* **3** (1961) 142.
28. W. W. MULLINS and R. F. SEKERKA, *J. Appl. Phys.* **35** (1964) 444.
29. J. A. BURTON, R. C. PRIM, and W. P. SLICHTER, *J. Chem. Phys.* **31** (1953) 15.
30. D. S. ROBERTSON and B. COCKAYNE, *J. Appl. Phys.* **37** (1966) 927.
31. M. A. WRIGHT, *J. Electrochem. Soc.* **112** (1965) 1114.
32. M. WEINSTEIN, R. O. BELL, and A. A. MENNA, *ibid* **111** (1964) 674.
33. R. S. WAGNER, W. C. ELLIS, K. A. JACKSON, and S. M. ARNOLD, *J. Appl. Phys.* **35** (1964) 2993.
34. N. HOLONYAK (JR), C. M. WOLFE, and J. S. MOORE, *Appl. Phys. Letters* **6** (1965) 64.
35. R. L. BARNS and W. C. ELLIS, *J. Appl. Phys.* **36** (1965) 2296.
36. J. D. FILBY and S. NIELSEN, *Brit. J. Appl. Phys.* **17** (1966) 81.
37. D. W. F. JAMES and C. LEWIS, *ibid* **16** (1965) 1089.
38. J. D. FILBY and S. NIELSEN, *Microelectronics and Reliability* **5** (1966) 11.
39. *Idem*, *J. Electrochem. Soc.* **112** (1965) 534.
40. *Idem*, *ibid*, 957.
41. H. P. BOKENKIRK, F. P. BUNDY, H. T. HALL, H. M. STRONG, and R. H. WENTORF, *Nature* **184** (1959) 1094.
42. A. A. GIARDINI and J. E. TYDINGS, *Amer. Mineralogist* **47** (1962) 1393.
43. J. M. GILLES and J. VAN CAKENBERGHE, *Nature* **182** (1963) 862.
44. *Idem*, *Solid State Phys. Electron., Telecomms. Internat. Conf. Brussels*, **2** (2) (1958) 900.
45. W. G. BURGERS, reference 3, p. 416.
46. T. B. REED and W. J. LAFLEUR, *Appl. Phys. Letters* **5** (1964) 191.